Gravity wave flux modulation by planetary waves in a circulation model

Ch. Jacobi, K. Fröhlich, A. Pogoreltsev

Zusammenfassung

Mit Hilfe eines Zirkulationsmodells der mittleren Atmosphäre wird die Ausbreitung der Quasi-Zwei-Tage-Welle simuliert. Das Modell verfügt über eine aktuelle Schwerewellenparametrisierung und ermöglicht daher die detaillierte Beschreibung der Wechselwirkung planetarer Wellen mit Schwerewellen. Bei Anwesenheit der Quasi-Zwei-Tage-Welle wird der Schwerewellenfluss mit der Periode von zwei Tagen und der räumlichen Struktur der Quasi-Zwei-Tage-Welle moduliert. Modellergebnisse zeigen, dass sich die Quasi-Zwei-Tage-Welle nicht gut in die untere Thermosphäre ausbreitet. Phasenvergleiche zwischen Quasi-Zwei-Tage-Welle und Divergenz des Eliassen-Palm-Flusses der Schwerewellen zeigen, dass dies eine Folge sekundärer Anregung der Quasi-Zwei-Tage-Welle durch brechende Schwerewellen ist, die außer Phase mit der Originalwelle erfolgt.

Abstract

The quasi-two-day wave is forced in a circulation model through adding an additional heating term in the troposphere with a period of about 2 days and a zonal wavenumber 3 Hough mode structure. The model contains an updated Lindzen-type gravity wave parameterisation that allows the formation of multiple breaking levels and thus the detailed description of interaction of gravity waves and planetary waves. In the presence of the two-day wave the gravity wave flux is modulated with the temporal and spatial structure of the wave. Model results show that the quasi-two-day wave does not propagate well to the lower thermosphere. Phase comparisons of the planetary wave and the gravity wave flux divergence show that the planetary wave and the gravity wave acceleration is out of phase in the mesosphere so that the modulated forcing of the background wind destructively interferes with the original planetary wave.

1. Introduction

The westward propagating quasi-two-day wave (QTDW) is one of the most prominent features of the atmosphere near solstice. This wave is a global planetary-scale oscillation, which is regularly observed by ground-based (e.g., Muller, 1972; Kalchenko and Bulgakov, 1973; Jacobi et al., 2001) and space-based techniques (e.g., Wu et al., 1996; Fritts et al., 1999; Lieberman, 1999). Its amplitude in winds may reach values up to 50 m/s (Craig et al., 1980) during Southern hemisphere summer, while Northern hemisphere amplitudes are usually lower, 30–50 m/s for the meridional component. From ground-based and space-based observations zonal wavenumbers s = 3 and s = 4 are inferred (Jacobi et al., 2001, Wu et al., 1996). For the Southern hemisphere the most prevailing 2-day wave has the zonal wavenumber s = 3.

The amplitude distributions of wind and temperature oscillations for the s = 3 QTDW are in good agreement with those of the normal Rossby-gravity mode. The occurrence of this wave in the course of one year and its amplification near solstice may be explained as the normal mode behaviour in the presence of summer jet instability (Salby and Callaghan, 2001). Plumb (1983a) suggested baroclinic instability of the summer easterly jet as a source of the strong

QTDW. Indeed, global circulation models (Norton and Thuburn, 1999; Mayr et al., 2001) have demonstrated the occurrence of strong QTDWs with s = 3 and s = 4 due to baroclinic and barotropic instability of the summer mesospheric jet.

To investigate the behaviour of the QTDW and its impact on the circulation under different conditions as well as its impact on the middle atmosphere circulation, simplified models are often used (Merzlyakov and Jacobi, 2004). However, simple circulation models not always produce a QTDW self-consistently, so that the wave structure has to be included in the model as an additional forcing (e.g. Palo et al., 1999; Fröhlich et al., 2003), usually near the lower boundary of the model. This means the QTDW is treated as a wave propagating from below, and is therefore subject to possible interaction with gravity waves (GWs). GWs are filtered in the middle atmosphere; therefore through non-zonal filtering by planetary waves (PWs) they are able to transport the signature of PWs upwards and possibly re-force these waves in the mesosphere (e.g. Smith, 1996). Modulation of GW flux through the QTDW has been proved by Manson et al. (2003) using a medium frequency radar network. On the other hand, numerical model results by Fröhlich et al. (2003) revealed wind amplitudes at summer midlatitudes that are smaller than known from measurements, and an influence of the GW amplitudes used for the GW parameterisation, indicating interaction of GW and QTDW in the model.

To investigate the possible influence of GW filtering through the QTDW on the propagation of the QTDW, we used a numerical 3D circulation model with a GW parameterisation based on the Lindzen (1981) approach, but with modifications that allow multiple breaking levels depending on the structure of the background circulation, so that a more realistic description of the planetary wave influence on GW propagation is possible.

2. Model description

The model is a 3D global grid point model based on the primitive equations in flux form, expressed in spherical coordinates in the horizontal and log-pressure coordinates $z = -H(\ln p/p_0)$ with H = 7 km in the vertical. The horizontal resolution is given in 36 latitudinal and 64 longitudinal points, referring to a 5°x5.625° mesh. The vertical domain consists of 48 layers extending from the ground to 135 km in log-pressure height, which is approximately 150 km in geometric height. The first grid point lies at 1.421 km, while Δz is defined as 2.842 km.

The governing equations base on those described by Rose (1983) and Jakobs et al. (1986). It includes a detailed radiation routine based on that of Berger and Dameris (1993), with several modifications as described in detail by Lange (2001). Dissipative and accelerating terms, such as Rayleigh friction, ion drag, eddy-diffusion and viscosity are added. Forcing via turbulent diffusion and molecular heat conduction is also included. Stationary planetary waves with zonal wavenumber 1 and 2 can be included as lower boundary conditions using a mean climatology from the 11-year Met Office analyses climatology. Additional planetary waves can be forced in the troposphere by the corresponding heating term.

The model equations are integrated numerically using the leapfrog-scheme. A numerical diffusive scheme is applied following Asselin (1972), which incorporates an approximate second-derivative time filter into the time integration cycle. The time interval for the dynamic equations is $\Delta t = 450$s. Solar radiation, the gravity wave parameterisation and the molecular conduction scheme are computed one time per hour, whereas the infrared radiation scheme is solved every 6 hours.

The GW parameterisation scheme follows the Lindzen approach that states that wave breaking occurs when the isentropes first become vertical $\partial\theta/\partial z = 0$, thus implying a loss of static stability and the onset of turbulence and mixing (see also Andrews et al., 1987). This assumption is implemented in the model, but taking into account possible multiple breaking levels and wave propagation between layers, where the wave is saturated, as well as heating/cooling effects due to GW dissipation. The parameterisation is based on the analytical solution (WKB approximation) of the vertical structure equation for the GW in the atmosphere with realistic arbitrary background wind and realistic radiative damping. The eddy diffusion coefficient is estimated using the idea of GW breaking due to instability proposed by Lindzen (1981).

In each GW time step, 48 waves are initialised, horizontally propagating in eight equally spaced directions, and six different phase speeds ranging from c = 5 to 30 m/s. All waves have the same horizontal wavelength λ_x =300 km and the amplitudes w_0 (given here in terms of the vertical velocity) are weighted by frequency and phase speed to provide a realistic spectrum W at the launch height z_0 = 10 km:

$$W(\omega, c, z = z_0) = w_0 c(\lambda) \frac{1}{1 + (\omega/\omega_0)^{\alpha}} \frac{1}{1 + (c/c_1)^{\beta} + (c_2/c)^{\gamma}} ,$$

where ω_0, α, β, γ, c_1, c_2 are coefficients as given in Gavrilov and Fukao (1999) and W is the spectrum at z = 0. In addition, a latitudinal and seasonal weighted term with increasing GW activity in the winter hemisphere is applied.

For the upward propagation of the gravity waves two processes have to be considered. The first is the filtering of the waves due to impinging the critical line of wind speed in the background flow and the second is the breaking process due to convective instability. If a wave is able to propagate upwards through the mean flow its amplitude grows due to decreasing density. To obtain their vertical structure a linearised set of equations describing the gravity waves is solved, first for the case without dissipation. Afterwards, a weak dissipation is introduced as a first order correction to the solution. Then, its vertical structure, the so-called WKB solution is written as follows:

$$W(z) = W(z = z_0) \sqrt{m(z = z_0)/m(z)}\, e^{\pm i \int_{z_0}^{z} m(z')dz'} e^{-\frac{1}{2}\int_{z_0}^{z} L(z')dz'} ,$$

where the vertical wavenumber squared is

$$m^2 = M - \frac{1}{4}L^2 - \frac{1}{2}\frac{\partial L}{\partial z}.$$

Assuming weak dissipation, i.e. taking dissipative terms to be small in comparison with 1/H, the operators L and M are:

$$L = -\frac{1}{H} + \frac{D(1+1/Pr)m^3}{\omega^+} + \frac{\alpha' m}{\omega^+}, \quad M = \frac{N^2 k^2}{\omega^{2+}} - \frac{1}{H\omega^+}\frac{\partial \omega^+}{\partial z} - \frac{1}{\omega^+}\frac{\partial^2 \omega^+}{\partial z^2},$$

where D is eddy diffusion, Pr is the Prandtl number set to Pr = 3 (Gavrilov and Yudin, 1992), $\omega^+ = \omega - k\ (\bar{u}\cos\varphi + \bar{v}\sin\varphi)$ the intrinsic angular frequency of the GW, α' is the Newtonian cooling coefficient, N^2 is Brunt Väisälä frequency squared, and k the horizontal wavenumber of the GW.

Wave overturning due to convective instability occurs if the wave amplitude exceeds a certain limit. In terms of the perturbed potential temperature θ' the breaking condition is $\left|\partial\theta'/\partial z\right| \geq \partial\overline{\theta}/\partial z$. This creates a convectively unstable situation and a transition from laminar to turbulent regime. To investigate the situation using the obtained analytical solution, we express this condition in terms of the perturbed vertical velocity w':

$$\left|\frac{\partial\theta'}{\partial z}\right| / \left|\frac{\partial\overline{\theta}}{\partial z}\right| = \frac{m|w'|}{\omega^{+}} \geq 1 .$$

Assuming that eddy diffusion limits the further increase in the wave amplitude with height, we obtain the saturation condition in the following form:

$$\frac{\partial}{\partial z}\left(\frac{m|w'|}{\omega^{+}}\right) = 0.$$

This conditions allows us to calculate the eddy diffusion coefficient from the set of equations and following Schoeberl et al. (1983) through

$$D = \frac{\omega^{+4}}{k^3 N^3 (1 + 1/\mathrm{Pr})}\left(\frac{1}{H} - \frac{\alpha' m}{\omega^{+}} - \frac{3}{\omega^{+}}\frac{\partial\omega^{+}}{\partial z}\right) .$$

Under breaking conditions GWs accelerate the mean flow due to vertical divergence of the vertical momentum flux. Usually, following the suggestions by Lindzen (1981), this force per unit mass is calculated using the obtained expressions for D and L and assuming that GW breaking conditions are given everywhere above the breaking level (Jakobs et al., 1986).

However, the background wind can substantially influence the propagation conditions of GWs (Pogoreltsev and Pertsev, 1995) and we have to expect the wave overturning only in some layers, where the breaking condition is satisfied (Akmaev, 2001). Especially this is important when the "mean" flow includes large-scale atmospheric waves with a short vertical wavelength (for instance, the diurnal tide). To take into account such possibility, we consider the divergence of the vertical momentum flux. The forcing per unit mass due to its divergence can be written as follows:

$$a_{GW} = -\frac{1}{\rho}\frac{\partial}{\partial z}(\rho\overline{u'w'}) = -\frac{1}{\rho}\frac{\partial}{\partial z}(\rho\frac{m\overline{w'^2}}{k}) = \frac{|w'|^2 m}{2k}(L + \frac{1}{H}).$$

To apply the Lindzen-type parameterisation of the GW drag to background conditions with a strong variability of zonal and meridional winds with altitude, we follow suggestions by Akmaev (2001). Stepping up from a given height level z, it is sufficient to calculate $|w'(z+\Delta z)|$ using the WKB solution with L taking into account some background dissipation – radiative damping in our case. Then $|w'(z+\Delta z)|$ is compared with the breaking value $|w'|_b = \omega^{+}/m$. If $|w'(z+\Delta z)|$ exceeds $|w'|_b$, it is reset to $|w'|_b$, the GW is assumed to break between z and $z+\Delta z$ and the forcing per unit mass is calculated by finite differences:

$$a_{GW}(z+\Delta z/2) = \frac{1}{2k}\left[\frac{m(z+\Delta z)\left|w'(z+\Delta z)\right|^2 + m(z)\left|w'(z)\right|^2}{2H}\right]$$
$$-\frac{1}{2k}\left[\frac{m(z+\Delta z)\left|w'(z+\Delta z)\right|^2 - m(z)\left|w'(z)\right|^2}{\Delta z}\right].$$

Otherwise, the wave is assumed to propagate free of breaking and acceleration of the mean flow is conditioned only by radiative damping of GWs. It should be noted, that in practice the GW levels are situated between the levels of the model and accelerations in zonal and meridional directions are calculated as $a_{GW\lambda} = a_{GW}\cos\vartheta, a_{GW\varphi} = a_{GW}\sin\vartheta$, where ϑ is the azimuth of GW propagation. Once obtained the breaking vertical velocity $\left|w'(z_b)\right|$ one can estimate more correctly the eddy diffusion coefficient by

$$D = \frac{\omega^+}{m^3(1+1/Pr)}\left[\frac{1}{H} - \frac{\alpha m}{\omega+} - 2\frac{\partial}{\partial z}\ln(m^{1/2}\left|w'\right|)\right],$$

which will be used to estimate the heating/cooling contribution of the GWs. To estimate the impact of GWs on the zonal mean temperature we follow suggestions by Schoeberl et al. (1983) and Plumb (1983b). The main idea is to use the thermodynamic equation and the energy conservation equation for gravity waves. Then, the total heating rate due to gravity wave dissipation can be written as follows:

$$Q_{GW} = -\frac{1}{\rho}\frac{\partial}{\partial z}\left(\rho\overline{w'T'}\right) - \left(1 + e_{wh}\frac{D}{\alpha + Dm^2/Pr}\right)\frac{\kappa}{H}\overline{w'T'},$$

where $\kappa = R/c_p$ and $e_{wh} \le 1$ is an efficiency of the mechanical energy conversion into heat. It should be noted that without dissipation $\overline{w'\theta'} = \overline{w'T'} = 0$ and GWs do not interact with the mean state. In our model we chose $e_{wh} = 1$.

3. Model experiments

Generally, the model runs start with a horizontally uniform temperature distribution, and during the first 90 days of the run the mean circulation establishes. During this phase the tides are filtered, in a second phase of 30 days the tides establish. In addition, where applicable, additional planetary waves are forced from then on. The results after the first two phases, i.e. from day 121 of the model run on, are analysed.

We performed 3 different model runs, each of them for July conditions, i.e. the model was run such that the radiative forcing conditions of day 122 are those for July 1. The first run (background run) includes the stationary wavenumber 1 from Met Office analyses, but no other planetary waves were included. Zonally averaged mean July zonal winds and temperatures are given in Figure 1. The summer hemisphere wind field is in reasonable good agreement with empirical models, while the winter middle atmosphere jet is too strong; this is partly due to the fact that in this run we neglect the stationary s = 2 planetary wave, as well as westward propagating planetary waves

In the second run (QTDW run), the QTDW is implemented into the model as a heating disturbance h_{2d} around the tropopause level after day 90. The forcing itself is smoothed in the

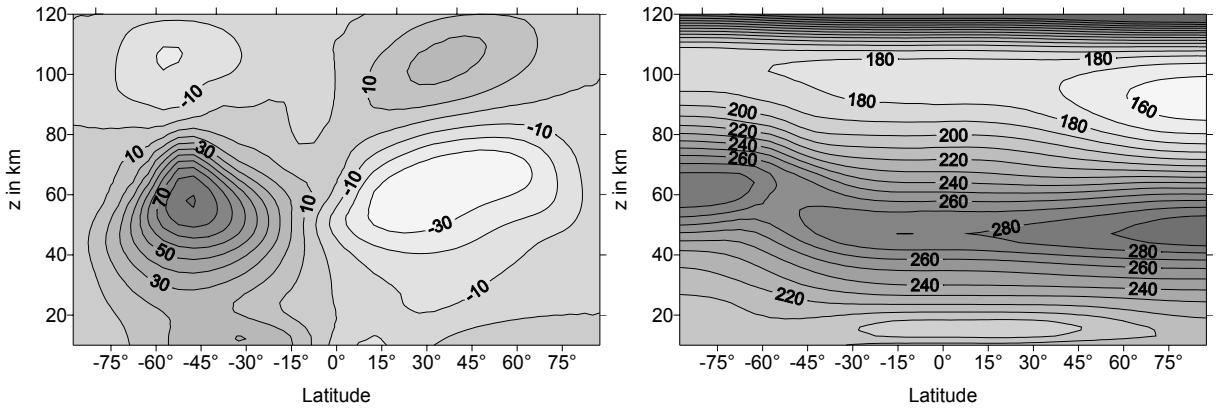

Figure 1: *Results of the reference run without additional planetary waves. Left panel : July mean zonally averaged zonal wind in ms^{-1}, positive eastward. Right panel: July mean zonally averaged temperature, values given in K.*

vertical domain with an exponential factor, and the disturbance term is defined by the properties of the wave

$$h_{2d} = A\Phi_{2d}(\varphi)\cos\left(2\pi s\frac{\lambda}{360°} - 2\pi\frac{t}{P}\right)\exp\left\{-\frac{(z-10)^2}{25}\right\},$$

with z given in km. A is the amplitude that is usually scaled to produce the values that are close to observations (Fedulina et al., 2004), $\Phi_{2d}(\varphi)$ is the latitudinal structure of the wave, obtained from Hough mode calculations for the Rossby-gravity wave (3,0), s = 3 is the zonal wavenumber, while P represents the period of the QTDW, which is here taken as P = 52.5 h, because this period gives the resonant response in the model. The minus sign in the cosine term gives a westward propagating wave. After day 121, the QTDW was modulated in amplitude with a period of 15 days to provide a reasonable description of the burst structure that is frequently observed. Figure 2 shows temperature amplitudes of the QTDW at 32.5°N for different heights. The bursts need about 2 weeks to propagate to the mesosphere.

The third run (GW filter run) essentially is the same as the QTDW run, but here after each GW parameterisation calculation we remove the s = 3 part from the gravity wave acceleration and heating terms. This set-up allows to analyse the effect that the modulated GW have on the s = 3 planetary wave.

3. QTDW Model results

The results of the QTDW run are presented in Figure 3. The data are averages over July so that the temperature amplitude structure (panel a) shows that the wave propagates to the mesosphere/lower thermosphere region in both hemispheres, with enhanced amplitudes in the summer hemisphere. The zonal wind amplitudes shown in panel (b) reveal small values compared to measurements, however, it can be seen that the wave propagates to higher northern hemisphere latitudes than it does in the southern hemisphere. Panel (c) of Figure 3 shows the Eliassen-Palm (EP) flux divergence per unit mass. The main effect of the wave consists in a negative (westward) acceleration of the summer hemisphere easterlies. The maximum values reach 6 ms^{-1}day^{-1}. Absolute values and the position of the region of maximum negative EP flux divergence are in good agreement with the experimental results by Lieberman (1999). The effect of the QTDW on the zonal mean wind is shown in panel (d) of Figure 3. The

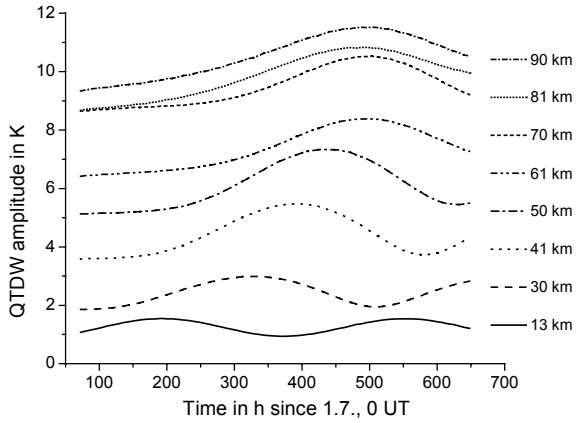

Figure 2: *QTDW temperature amplitudes at different heights at 32.5°N. The curves are shifted by 1 ms^{-1} relative to each other.*

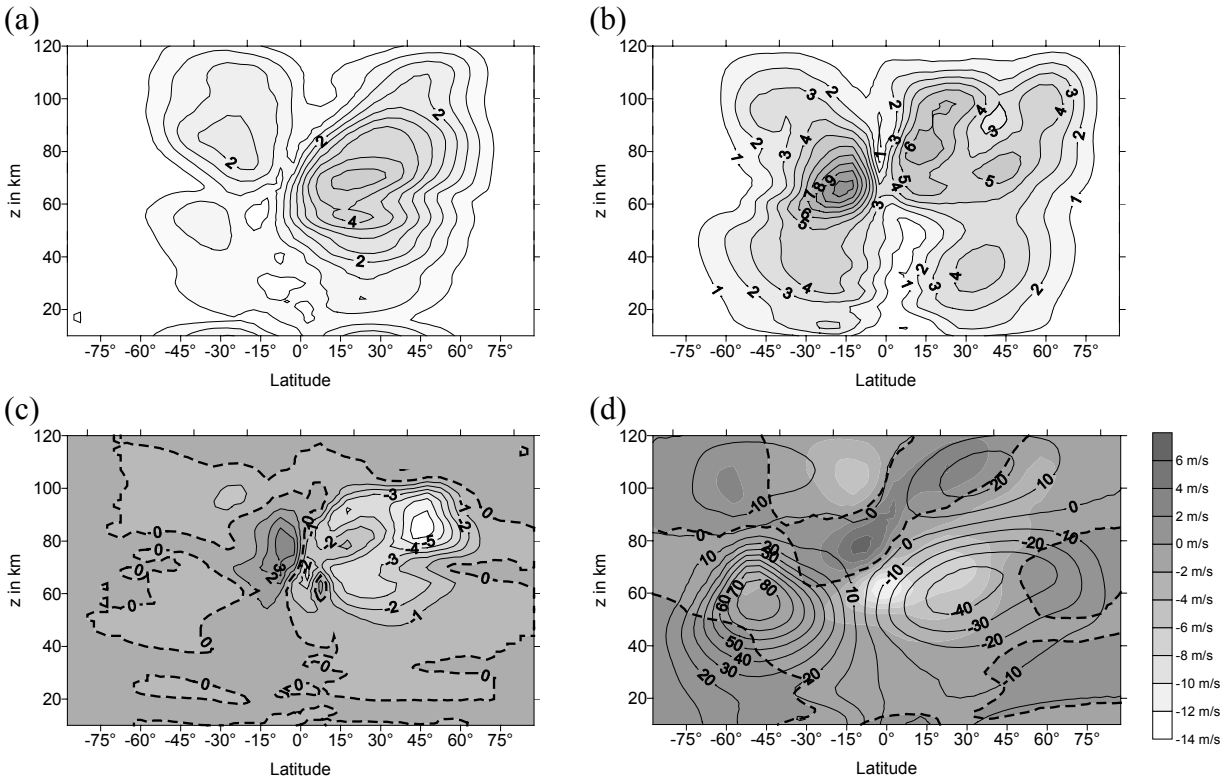

Figure 3: *July mean results of QTDW simulation (a) temperature amplitudes in K, (b) zonal wind amplitudes in m/s, (c) Eliassen-Palm-flux divergence per unit mass in ms^{-1}day^{-1} and (d) zonal mean wind in m/s, given as contours together with the differences between the reference run and this result, shown as greyscaling.*

QTDW acceleration of the mean flow increases the mesospheric jet. This is in accordance with measurements (Jacobi, 1998), but from the measurements alone one cannot infer whether the QTDW influences the mean circulation or changes in mean circulation lead to increased forcing of the QTDW. Merzlyakov and Jacobi (2004) have tested the stability of the mean circulation under the assumption of stronger mesospheric jets and found that very strong jets

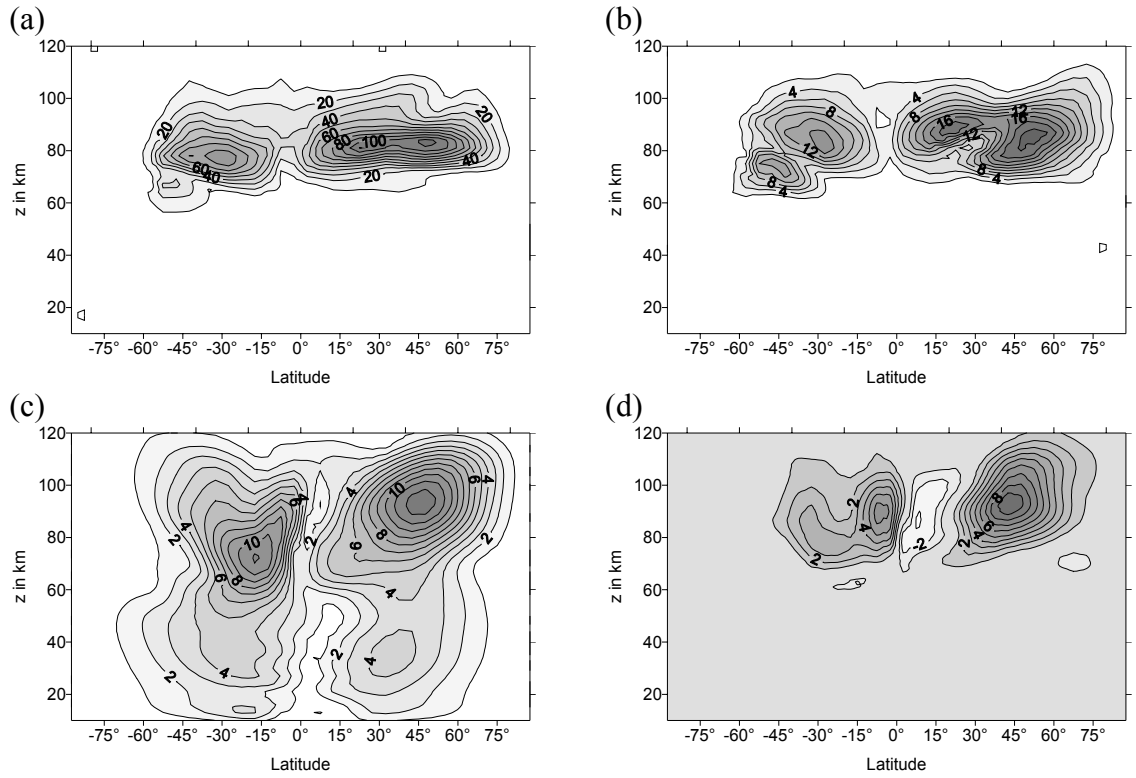

Figure 4: *July mean GW flux in m^2s^{-2} (a) and GW flux divergence in $ms^{-1}day^{-1}$ (b). Only the components with s = 3 and P = 52.5 h are displayed here. Panel (c) displays the QTDW zonal wind amplitude, after the GW acceleration and heating with s = 3 was removed after each time step, while (d) shows the differences between (c) and the original amplitude shown in Figure 3(b).*

lead to instability resulting in a QTDW. Here, the wave is explicitly forced, and instability does not play a role.

To estimate the GW effect on the propagation of the QTDW, we isolated the component of the GW flux with the same longitudinal and temporal structure of the QTDW, i.e. only the GW planetary wave modulation with s = 3 and P = 52.5 h is displayed in Figure 4. Panel (a) shows the amplitude of this GW flux modulation. The acceleration of the background flow due to this modulation, given in $ms^{-1}day^{-1}$, is shown in panel (b). Note that this acceleration only acts to increase or decrease the QTDW, or shifts its phase, but has no direct influence on the mean circulation. Panel (c) of Figure 4 shows the zonal wind amplitudes of the QTDW after removing the GW s = 3 and P = 52.5 h GW flux component in the GW filter run. The amplitudes are considerably stronger than those presented in Figure 3(b).

The differences between the zonal wind amplitudes of the GW filter run and the QTDW run are displayed in Figure 4(d). Except for a small region near the equator the difference is positive, i.e. removing the GW modulation leads to a strong increase of the wave. In turn, this means that the GW flux modulation and subsequent GW breaking in the mesosphere decreases the amplitude of the original wave, which requires that the modulation of the GW flux divergence and the QTDW are in or near antiphase in the region of strong GW breaking. As an example, in Figure 5 we show QTDW phases and the phase of the GW s = 3 and P = 52.5 h GW flux component at 32.5°N for 2 different heights, representing the 2 maximum

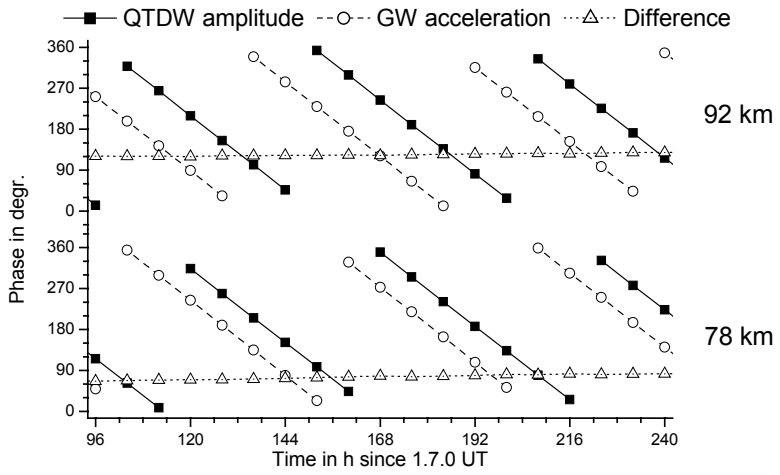

Figure 5: *Phases of QTDW amplitudes (black squares), GW acceleration (open circles) and their differences (open triangles) at 92 km (upper panel) and 78 km (lower panel), at 32.5°N.*

heights of GW divergence visible in Figure 4(b). The two "waves" are not in phase, but while the phase difference at 78 km is near quadrature, it is clearly above 90° near 92 km. Therefore, we may conclude that at least near 90 km the QTDW is suppressed by the modulated GW forcing.

We present the time series for 32.5°N in Figure 6. Panel (a) shows the result for the QTDW run, with the GW flux and GW acceleration shown in panels (b) and (c). The two maxima of GW flux divergence are visible in panel (c). The phase differences for all heights are shown in Figure 6(d). In the lower mesosphere, QTDW and GW acceleration are in phase, while the differences increase with height. Above about 70 km the phase difference exceeds 90°, so that the modulated GW flux divergence leads to a suppression of the wave. Figure 6(e) shows the QTDW zonal wind amplitude in the GW filter run. The amplitudes are considerably larger than in the QTDW run, see also Figure 4(b). The differences amount to up to 9 ms^{-1} (Figure 6(f)). Note that only the s = 3 part of the GWs is responsible for the wave suppression, while the GW-spectrum in total provides a waveguide for the QTDW via interaction with the zonal mean wind. If the GW parameterisation is replaced by pure Rayleigh friction (not shown here) the QTDW reaches only mesospheric heights and is not able to propagate into the thermosphere. Also, the experiments of Norton and Thuburn (1999) showed that the development of the QTDW depended on the parameterisation of gravity waves. Similar results were obtained by Meyer (1999); however he concluded that the QTDW in the thermosphere develops from interaction between GWs and the mesospheric QTDW.

4. Conclusions

Using a simple circulation model with an updated Lindzen-type GW parameterisation, we analysed the propagation of the QTDW into the mesosphere. We forced the QTDW as a heating disturbance near the tropopause. Therefore, the wave interacts with the gravity waves, and modulate the GW flux with the wavenumber and period of the QTDW. Comparing the modulation of the GW flux and the QTDW phases, it is evident that the modulated GW acceleration of the mean flow suppresses the QTDW in the mesosphere.

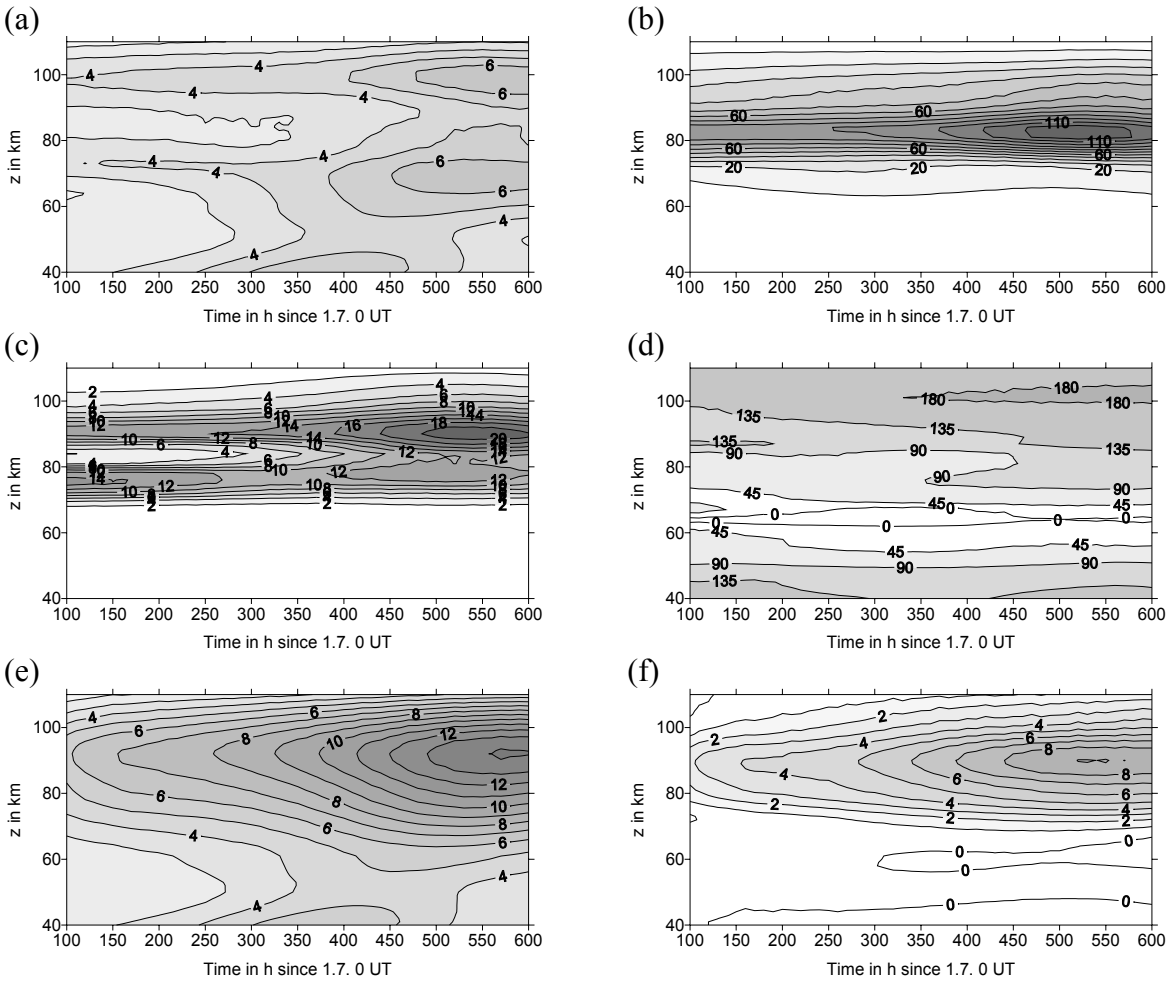

Figure 6: *Time series at 32.5°N: (a) zonal wind amplitude of the QTDWin ms^{-1}, (b) GW flux component with s = 3 and P = 52.5 in m^{2}s^{-2}, (c) GW acceleration component with s = 3 and P = 52.5 in ms^{-1}day^{-1}, (d) phase difference in degree between zonal wind amplitude and GW acceleration, (e) same as (a), but after the s = 3, P = 52.5 h component was filtered from the GW acceleration and heating, (f) difference between (d) and (a).*

We have to take into account that the approach chosen is somewhat arbitrary. First, from theory and observations it is not necessarily justified that the QTDW is forced in the lower model regions. However, if we introduce a forcing in situ, GW-QTDW interaction will not take place or will be reduced. Second, the interaction of the waves is described using a GW parameterisation with partly unrealistic assumptions, as instantaneous propagation. On the other hand, measurements (Manson et al., 2003) show that a QTDW modulation of GW exists in the mesosphere. Therefore we may conclude that the suppression of planetary waves propagating from below through modulated GW breaking is a possible factor that may affect planetary wave propagation.

Acknowledgements

This study was supported by Bundesministerium für Bildung und Forschung within AFO2000 under grant 07ATF10 (MEDEC). We thank the COMMA working group, Cologne, for providing us with the basic version of the model.

References

Akmaev, R.A., 2001. Simulation of large scale dynamics in the mesosphere and lower thermosphere with Doppler-spread parameterization of gravity waves. 2. Eddy mixing and the Diurnal Tide. Journal of Geophysical Research 102, 1203-1205.

Andrews, R.A., Holton, J., Leovy, C., 1987. Middle Atmosphere Dynamics. Academic Press, Orlando.

Asselin, R., 1972. Frequency filter for time integrations. Mon. Wea. Rev. 100, 487-490.

Berger, U., Dameris, M., 1993. Cooling of the upper atmosphere due to CO2 increases: a model study. Annales Geophysicae 11, 809-819.

Craig, R.L., Vincent, L.A., Fraser, G.J., Smith, M.J., 1980. The quasi 2-day wave near 90 km altitude at Adelaide (350S). Nature 287, 319-320.

Fedulina I.N., Pogoreltsev, A.I., Vaughan, G., 2004. Seasonal, interannual and short-term variability of planetary waves in Met Office stratospheric assimilated fields. Quarterly Journal of the Royal Meteorological Society 130, 2445-2458.

Fritts, D.C., Isler, J.R., Lieberman, R.S., Burrage, M.D., Marsh, D.R., Nakamura, T., Tsuda, T., Vincent, R.A., Reid, I.M.,1999. Two-day wave structure and mean flow interactions observed by radar and High resolution Doppler Imager. Journal of Geophysical Research, 104, 3953-3969.

Fröhlich, K., Pogoreltsev, A., Jacobi, Ch., 2003. Numerical simulation of tides, Rossby and Kelvin waves with the COMMA-LIM model. Advances in Space Research 32, 863-868, doi:10.1016/S0273-1177(03)00416-2.

Gavrilov, N.M., Yudin, V.A., 1992. Model for coefficients of turbulence and effective Prandtl Number produced by breaking gravity waves in the upper atmosphere. Journal of Geophysical Research 97, 7619-7624.

Gavrilov, N.M., Fukao, S, 1999. A comparison of seasonal variations of gravity wave intensity observed with the middle and upper atmosphere radar with a theoretical model. Journal of Atmospheric Sciences 56, 3485-3494.

Jacobi, Ch., 1998: On the solar cycle dependence of winds and planetary waves as seen from midlatitude D1 LF mesopause region wind measurements. Annales Geophysicae 16, 1534-1543.

Jacobi, Ch., Yu.I. Portnyagin, E.G. Merzlyakov, B.L. Kashcheyev, A.N. Oleynikov, D. Kürschner, N.J. Mitchell, H.R. Middleton, H.G. Muller and V.E. Comley, 2001: Mesosphere/lower thermosphere wind measurements over Europe in summer 1998. Journal of Atmospheric and Solar-Terrestrial Physics 63, 1017-1031.

Jakobs, H.J., Bischof, M., Ebel, A., Speth, P., 1986. Simulation of gravity wave effects under solstice conditions using a 3-D circulation model of the middle atmosphere. Journal of Atmospheric and Terrestrial Physics 48, 1203-1223.

Kalchenko, B.V., Bulgakov S.V., 1973. Study of periodic components of wind velocity in the lower thermosphere above the equator. Geomagnetism Aeronomy 13, 955-956.

Lange, M., 2001. Modellstudien zum CO2-Anstieg und O3-Abbau in der mittleren Atmosphäre und Einfluss des Polarwirbels auf die zonale Symmetrie des Windfeldes in der Mesopausenregion. Reports of the Institute for Meteorology 25, University of Leipzig, 121 p.

Lieberman, R.S., 1999. Eliassen-Palm fluxes of the two-day wave. Journal of the Atmospheric Sciences 56, 2846-2861.

Lindzen, R.S., 1981. Turbulence and stress owing to gravity wave and tidal breakdown. Journal of Geophysical Research 86, 9709-9714.

Manson, A.H., Meek, C.E., Luo, Y., Hocking, W.K., MacDougall, J., Riggin, D., Fritts, D.C., Vincent, R.A., 2003. Modulation of gravity waves by planetary waves (2 and 16 d): observations with the North American-Pacific MLT-MFR radar network. Journal of Atmospheric and Solar-Terrestrial Physics 62, 85-104.

Mayr, H.G., Mengel, J.G., Chan, K.L., Porter, H.S., 2001. Mesosphere dynamics with gravity wave forcing: Part II. Planetary waves. Journal of Atmospheric and Solar-Terrestrial Physics 63, 1865-1881.

Meyer, C.K., 1999. Gravity wave interactions with mesospheric planetary waves: A mechanism for penetration into the thermosphere-ionosphere system. Journal of Geophysical Research 104, 28181-28196.

Merzlyakov, E.G., Jacobi, Ch., 2004. Quasi-two-day wave in an unstable summer atmosphere – some numerical results on excitation and propagation. Annales Geophysicae 22, 1917-1929.

Muller, H.G., 1972. Long-period meteor wind oscillations, Philosophical Transactions of the Royal Society of London A271 (1217), 585-598.

Norton, W.A., Thuburn, J., 1999. Sensitivity of mesospheric mean flow, planetary waves and tides to strength of gravity wave drag. Journal of Geophysical Research 104, 30897-30911.

Palo, S.E., Roble, R.G., Hagan, M.E., 1999. Middle atmosphere effects of the quasi-two-day wave determined from a General Circulation Model. Earth, Planets, and Space 51 (7-8), 629-647.

Plumb, R.A., 1983a. Baroclinic instability of the summer mesosphere: A mechanism for the quasi-two-day wave? Journal of Atmospheric Sciences 40, 262-270.

Plumb, R.A., 1983b. A new look on the energy cycle. Journal of the Atmospheric Sciences 40, 1669-1688.

Pogoreltsev, A.I., Pertsev, N.N., 1995. The influence of background wind on the formation of the acoustic-gravity wave structure in the thermosphere. Izvestiya Akademii Nauk Fizika Atmosfery i Okeana 31 (6), 755-760.

Rose, K., 1983: On the influence of non-linear wave-wave interaction in a 3-d primitive equation model for sudden stratospheric warmings. Beitr. Phys. Atm. 56, 14-41.

Salby, M.L., Callaghan, P.F., 2001. Seasonal amplification of the 2-day wave: relationship between normal mode and instability. Journal of the Atmospheric Sciences 58, 1858-1869.

Schoeberl, M.F., Strobel, D.F., Apruzese, J.P., 1983. A numerical model of gravity wave breaking and stress in the mesosphere. Journal of Geophysical Research 88, 5249-5259.

Smith, A.K., 1996. Longitudinal variations in mesospheric winds: evidence for gravity wave filtering by planetary waves. Journal of the Atmospheric Sciences 53, 156-1173.

Wu, D.L., Fishbein, E.F., Read, W.G., Waters, J.W., 1996. Excitation and evolution of the quasi-2-day wave observed in UARS/MLS temperature measurements. Journal of the Atmospheric Sciences 53, 728-738.

Addresses:

Christoph Jacobi, Kristina Fröhlich, Institute for Meteorology, University of Leipzig, Stephanstr. 3, 04103 Leipzig, Germany, jacobi@uni-leipzig.de

Alexander I Pogoreltsev, Russian State Hydrometeorological University, Maloohtinsky 98, St. Petersburg 195196, Russia